X-ray and γ-ray emissions from millisecond pulsars

Jumpei Takata

(The University of Hong Kong)

Collaborators

Theory;

K.S. Cheng, Y. Wang (HKU), R.E. Taam (ASIAA, Taiwan)

Observation;

A. Kong, R.H. Huang, T.Tam, J. Wu (Natinal Tuing Hua University, Taiwan),

D.Hui (Chungnang University, Korea),

E.Wu (HKU)

- My first text book on pulsars
- Cover picture; Hα bow shock nebula of black widow pulsar PSR B1957+20.
- Chapters 4,5 introduce basic idea of MPSs.

Contents

1, Introduction

- Pulsars are rotating and strongly magnetized objects.
- >2000 pulsars are detected

-Spin down dipole magnetic field

$$B_d(\text{Gauss}) = 3.2 \times 10^{19}(P\dot{P})^{1/2}$$

-Spin down age

$$\tau(\text{yr}) = P/(2\dot{P})$$

- MSPs (~100) are relatively old, weakly magnetized and rapidly rotating pulsars.
- ～115 γ-ray pulsars (～40 MSPs)

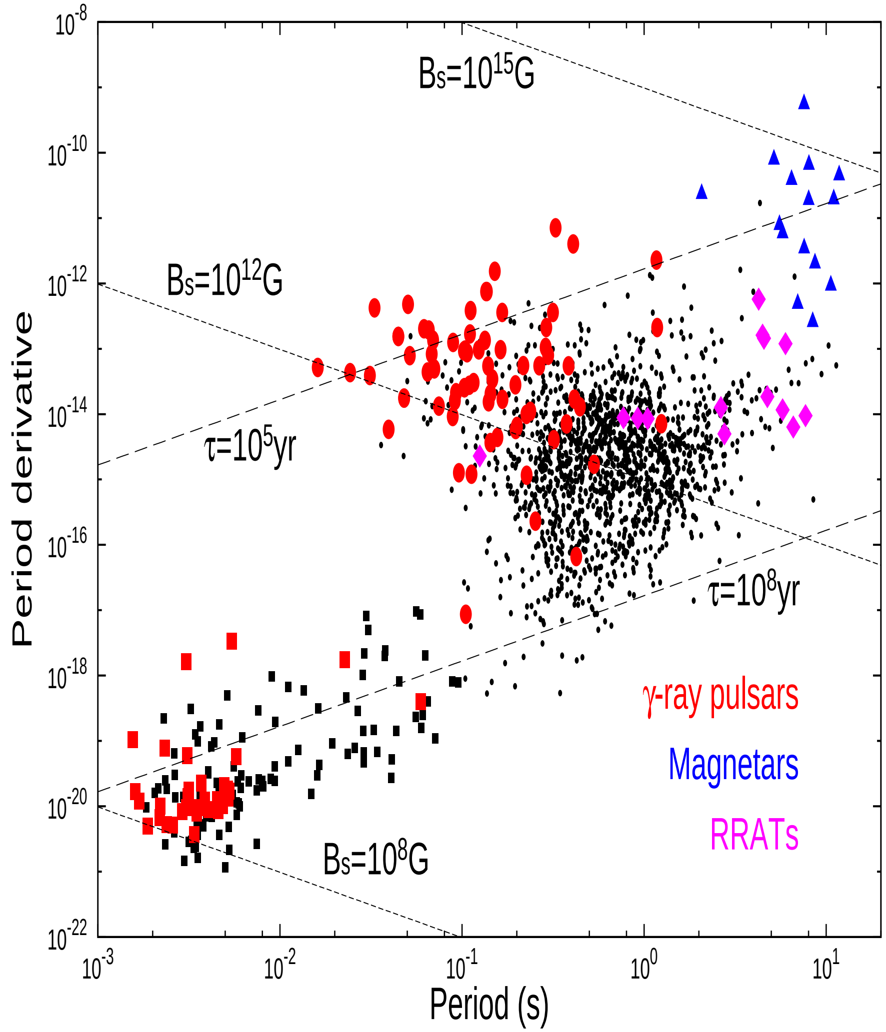

Fermi first pulsar catalog (Abdo et al. 2010, *ApJS*)

- *Fermi*-LAT six month observations detected pulsed emissions from 46 pulsars (22 radio-loud pulsars, 16 radio-quiet pulsars, and 8 radio-loud MSPs)

6 radio -loud, 1 radio-quiet, and no MSPs in *EGRET* era.

- Double peak and energy dependent γ-ray profiles
- Power low plus exponential cut-off spectrum (E_{cut}~0.5-8 GeV)

Vela **Pulse profile**

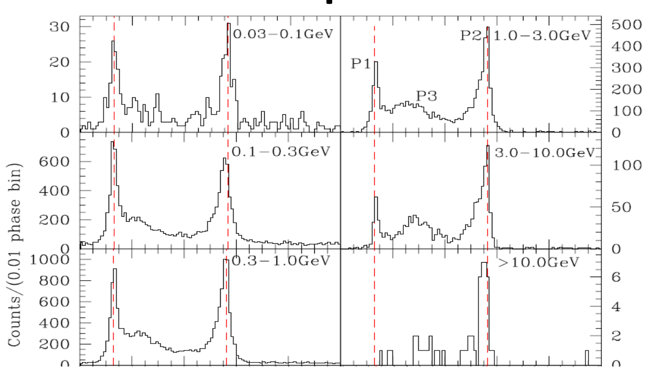

Spectrum

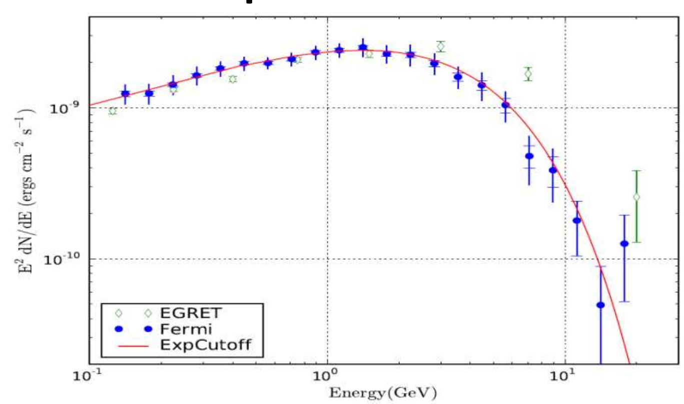

- Second pulsar catalog (3 yr data) will include 117 pulsars.

-Radio-loud, 41; radio-quiet, 36;

-Radio-loud MSPs 40 (binary : isolated ～ 1: 0.4)

γ-ray MSPs

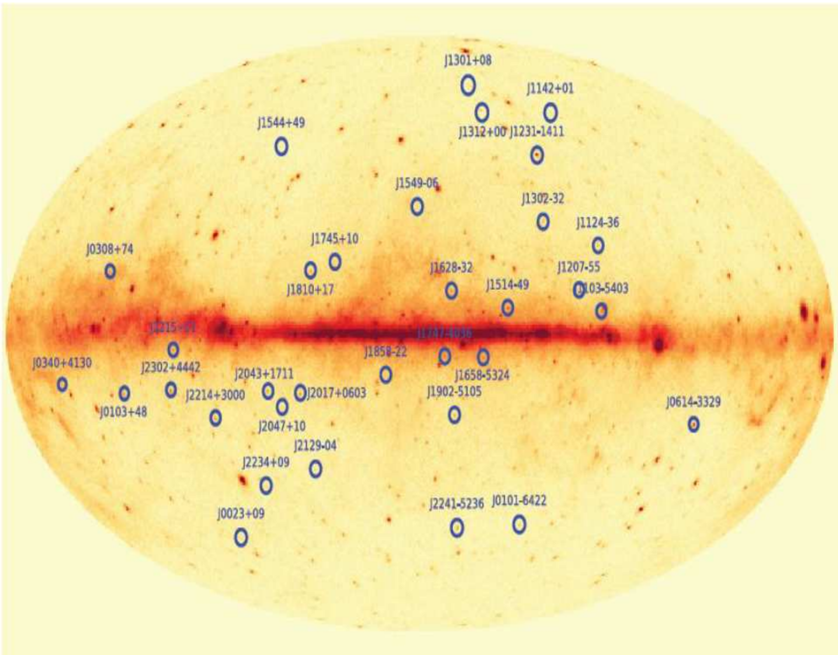

- ❑ Initially, most of them are *Fermi* un-ID sources.
- ❑ Follow up radio observations discovered radio MSPs.
- ❑ Using the timing parameters, the pulsed γ-rays were confirmed.

MSPs are major contributor to the Galactic γ-ray sources

It could be more than the normal pulsars (Takata et al. 2011 *MNRAS*)

Pulsed light curve
-Phase relation between Radio and γ-ray

Class I
gamma-ray profile lags radio

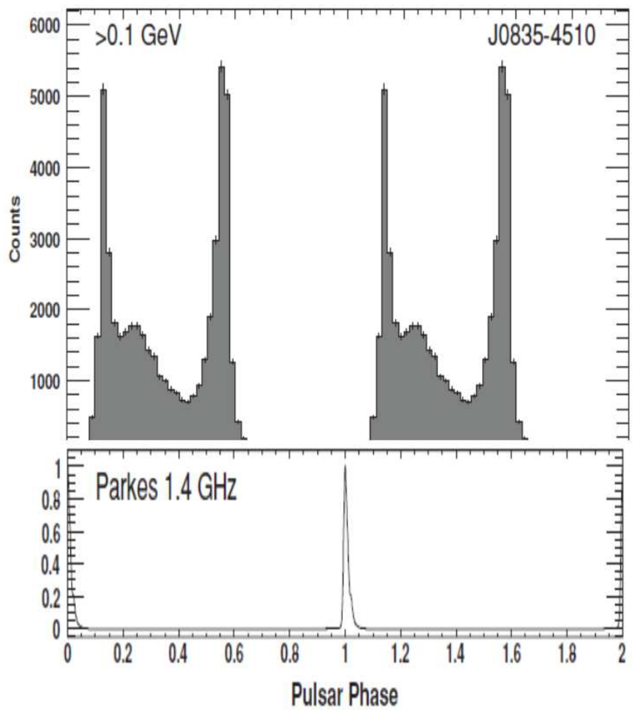

Majority gamma-ray pulsars
~100
10 MSPs

Class II
phase-aligned peaks

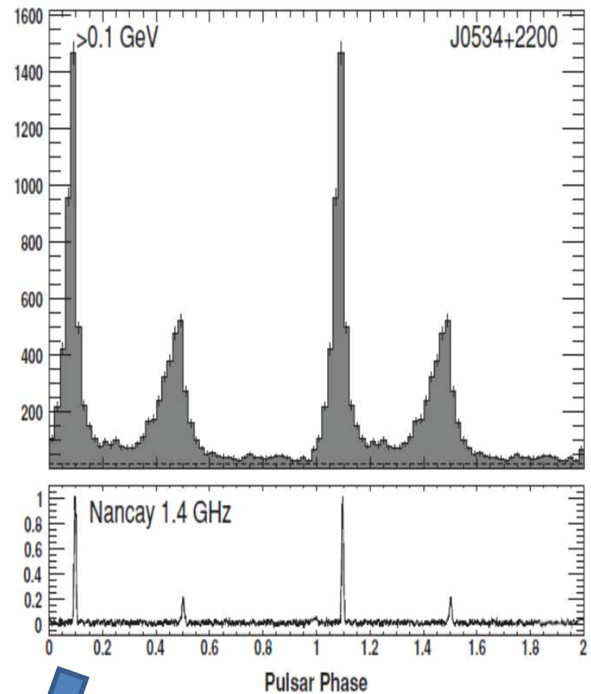

Crab

4MSPs (including PSR B1937+21, exhibiting giant pulse)

γ and radio come from same region

Class III
gamma-ray profile precedes radio

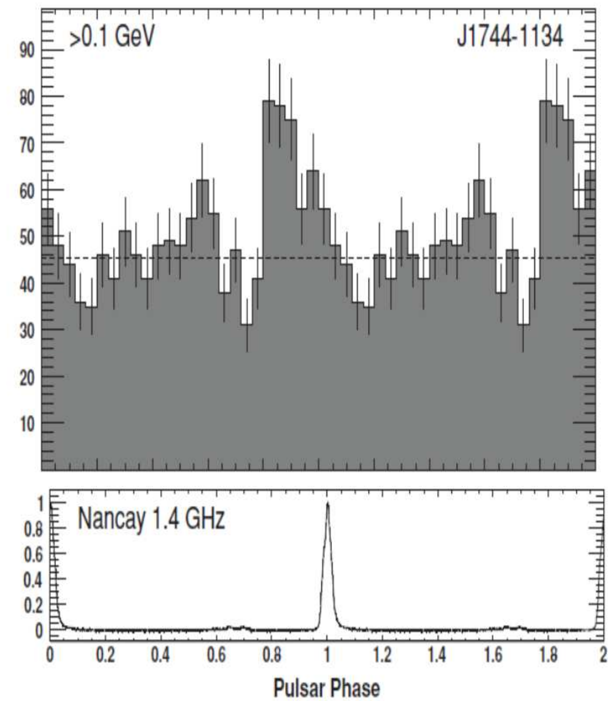

2MSPs

Emission models

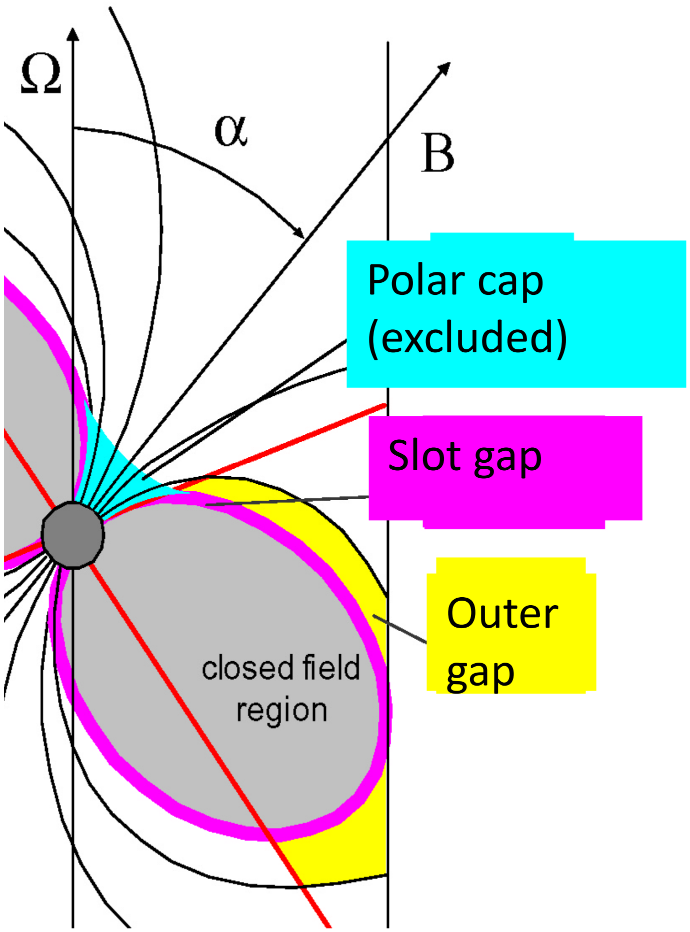

- Pulsar as unipolar inductor

$$V_a = 1.3 \times 10^{13} P^{-3/2} \dot{P}_{-15}^{1/2} \text{ Volt}$$

- $E_{||}$ arises in the charge depletion region (gap) from Goldreich-Julian charge density $\rho_{GJ} = \vec{\Omega} \cdot \vec{B}/2\pi c$

$$\nabla \cdot \mathbf{E} = 4\pi\,(\rho - \rho_{GJ})$$

- $E_{||}$ accelerates electrons/positrons to $\Gamma > 10^7$.
- Curvature radiation can produce ~GeV γ-rays

Pulsar magnetosphere

- Charged separated magnetosphere (Goldreich & Julian 1969)

  - Force free condition implies Goldreich-Julian charge density

$$E + \frac{(\Omega \times r)}{c} \times B = 0 \Rightarrow \rho = \frac{\nabla \cdot E}{4\pi} = \frac{-\Omega \cdot B}{2\pi c} \frac{1}{[1 - (\Omega r/c)^2 \sin^2 \theta]}$$

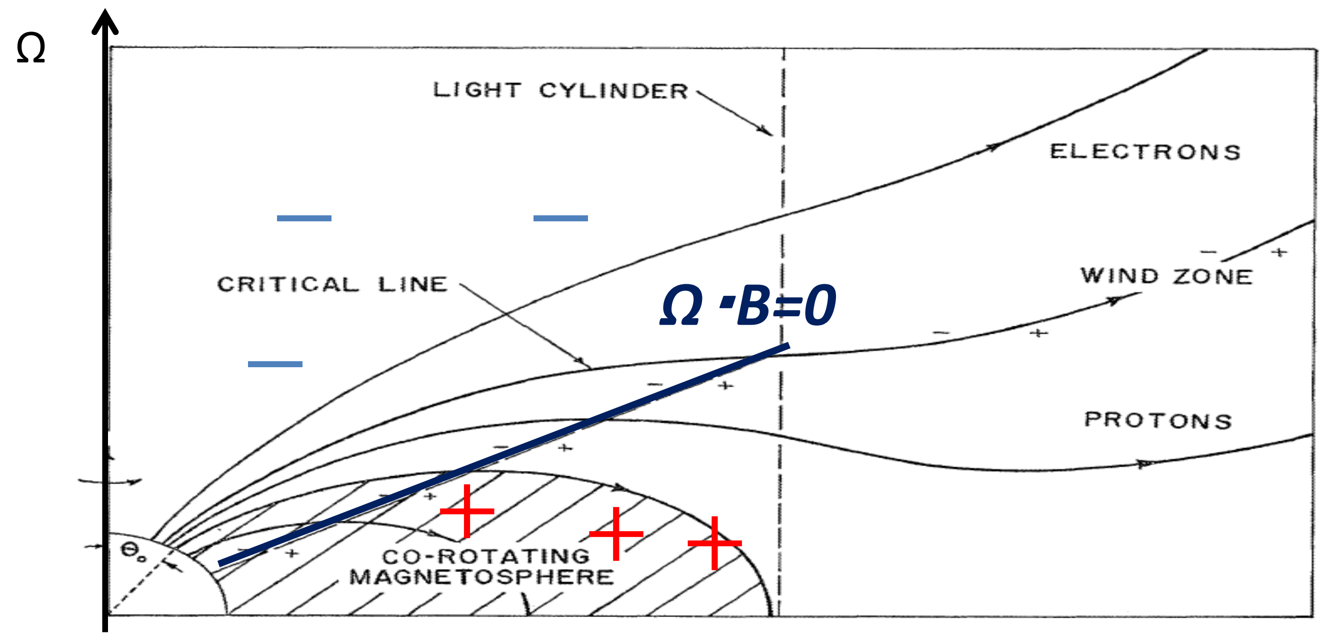

-No electric field along the magnetic field and no acceleration.

Particle simulation for pulsar magnetosphere

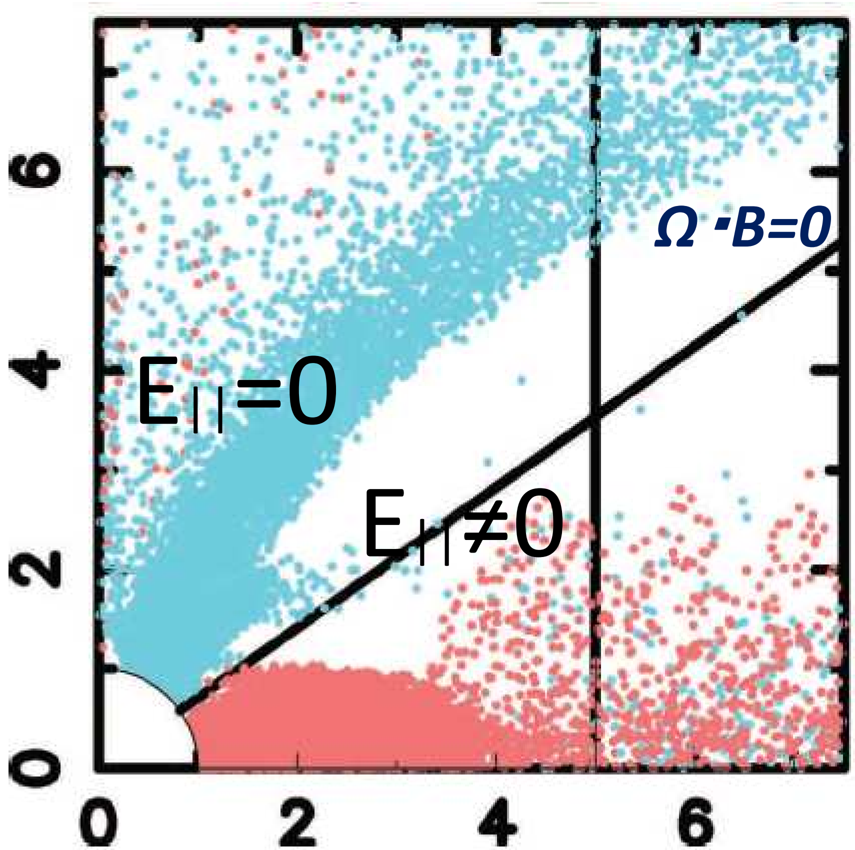

(Wada & Shibata 2007, 2011, *MNRAS*)

- ❑ Charge starved region, where $E_{||} \neq 0$, develops around the null charge surface.
- ❑ It is more likely that the outer gap exists in the outer magnetosphere.
- ❑ Co-existence of slot gap and outer gap in the magnetosphere.
  (Yuki & Shibata, 2012, *PASJ*)

2, Outer gap prediction

- γ-ray luminosity $L_\gamma \sim I(\mathrm{current}) \times \Phi_{nco}$ (Potential)
- In general, $I \propto D_\perp$ and $\Phi_{nco} \propto (D_\perp)^2$ $D_\perp$; gap thickness at the light cylinder

$$L_\gamma \sim f^3 L_{sd} = 3.8 \times 10^{35} f^3 (P/1\mathrm{ms})^{-4} (B_d/10^8\mathrm{G})^2 \mathrm{erg\ s}^{-1}$$

$$f=(D_\perp/R_{lc})$$

- The high-energy photons emitted in the gap can become pairs by

  GeV γ + X (back ground)→ $e^\pm$ (photon-photon pair-creation in the gap)

or

  GeV γ + B→$e^\pm$ (magnetic pair-creation near the surface)

- These pairs limit the growth of the outer gap, and hence determine the gap thickness and γ-ray luminosity.

$D_\perp$ and L_γ; photon-photon pair-creation

- MSPs exhibit thermal X-ray radiation with a temperature of $T_r \sim 10^6$ K and an effective radius of $R_r \sim 0.1$-1km
- Heated polar cap by incoming particles and γ-rays
  - Temperature (X-ray flux = flux of incoming particles from the gap)

$$T_r \sim 1.4\times10^6 f^{1/4}(L_{sd}/10^{34}\mathrm{erg\ s^{-1}})^{5/48}(B_d/10^8\mathrm{G})^{1/24}\mathrm{K}$$

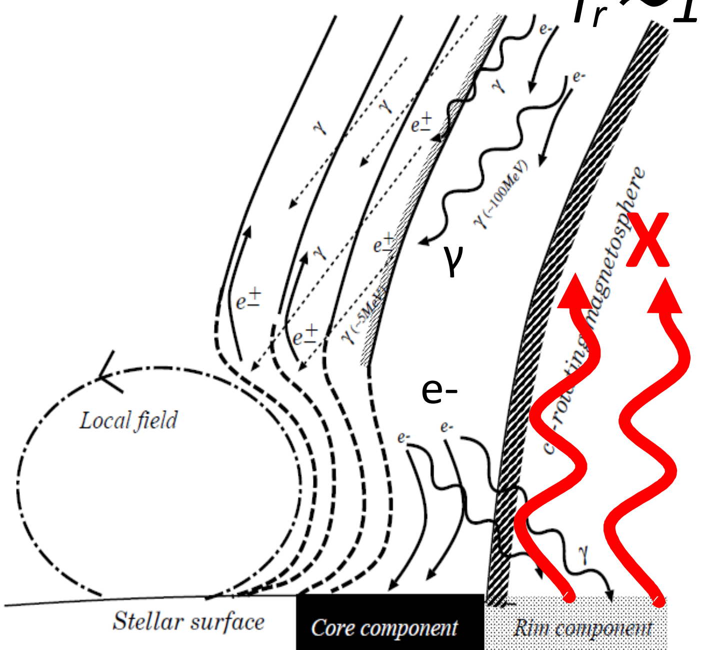

Polar cap

(Takata et al., 2012, *ApJ*)

- Energy of curvature radiation in the gap

$$E_c \sim 25 f^{3/2}(P/1\mathrm{ms})^{3/2}(B_d/10^8\mathrm{G})^{3/4}\mathrm{GeV}$$

- Pair-creation condition

$$E_c \times (3kT_r) = (m_e c^2)^2$$

Rc; curvature radiation

$$f \sim 0.3(L_{sd}/10^{34}\mathrm{erg\ s^{-1}})^{-13/42}(B_d/10^8\mathrm{G})^{1/21}$$

$f=(D_\perp/R_{lc})$

$$L_\gamma \sim f^3 L_{sd}$$

$$L_\gamma^p \sim 3\times10^{32}(L_{sd}/10^{34}\mathrm{erg s^{-1}})^{1/14}(B/10^8\mathrm{G})^{1/7}(R_c/R_{lc})^{1/7}(R_r/1\mathrm{km})^{2/7}\mathrm{erg\ s^{-1}}$$

Insensitive to pulsar parameters

$D_\perp$ and L_γ; magnetic pair-creation

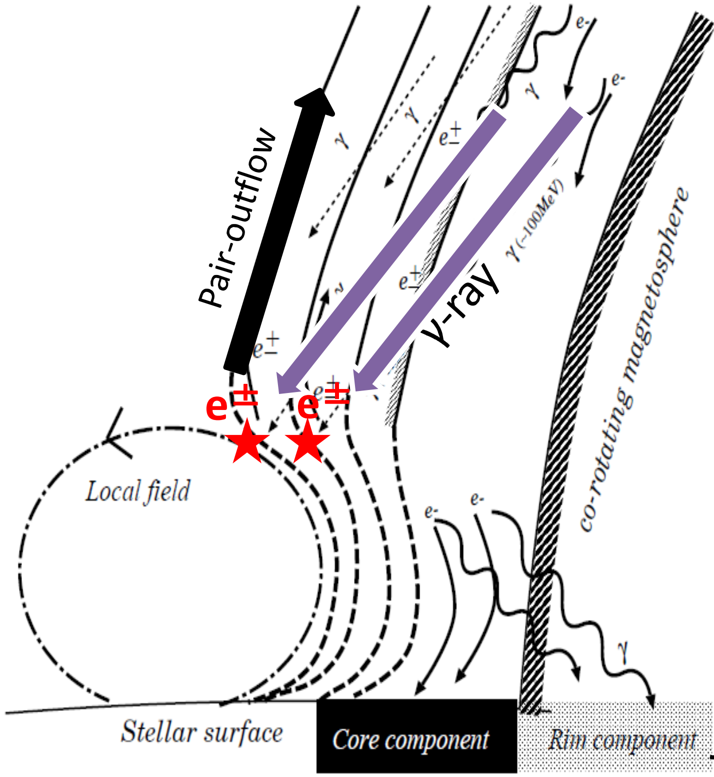

- Near the stellar surface, multipole magnetic field could dominate the dipole fields $B_s \sim 10 - 100 B_d$
- Magnetic pair-creation of incoming γ-rays.
- If the multipole magnetic field bends the global dipole field, the created pairs can flow back to outer magnetosphere, and limit the size of the outer gap (Takata et al. 2010, *ApJ*).

$$f \sim 0.4K(L_{sd}/10^{34}\mathrm{erg\ s^{-1}})^{-1/8}(B_d/10^8\mathrm{G})^{1/4}$$

$$K \sim (B_s/10^{11}\mathrm{G})^{-2}(s_c/10^6\mathrm{cm})$$

Bs; local magnetic field
Sc; local curvature radius

$$L_\gamma^m \sim 6\times 10^{32} K^3 (L_{sd}/10^{34}\mathrm{ergs^{-1}})^{5/8}(B/10^8\mathrm{G})^{3/4}\mathrm{erg\ s^{-1}} \quad \longleftarrow \quad L_\gamma \sim f^3 L_{sd}$$

Predictions vs. Observations

L_γ vs. L_{sd}

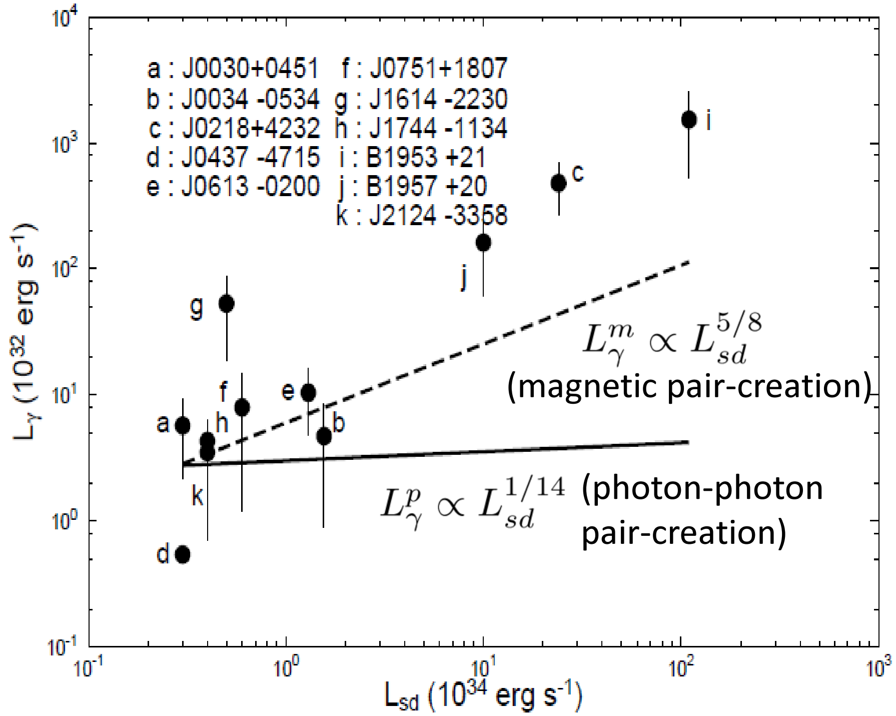

L_γ vs. τ

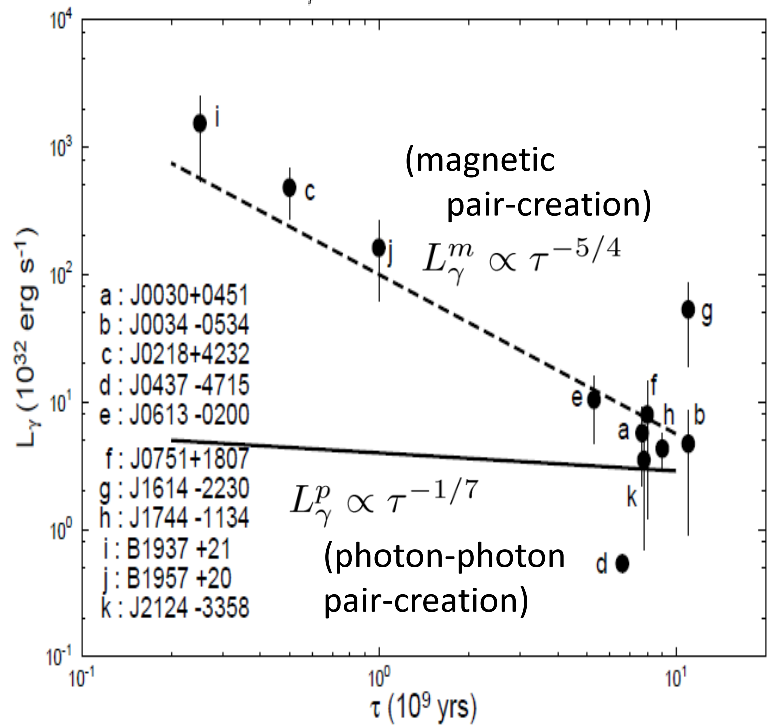

- ❑ The outer gap closed by the magnetic pair-creation process is preferred over the photon-photon pair-creation model.
- ❑ By fitting the observed spectra, we suggested (Wang et al. 2010, *ApJ*)

1, for $L_{sd} > 10^{36}$ erg/s, the photon-photon pair-creation controls the gap,

2, for $L_{sd} < 10^{36}$ erg/s, the magnetic pair-creation controls.

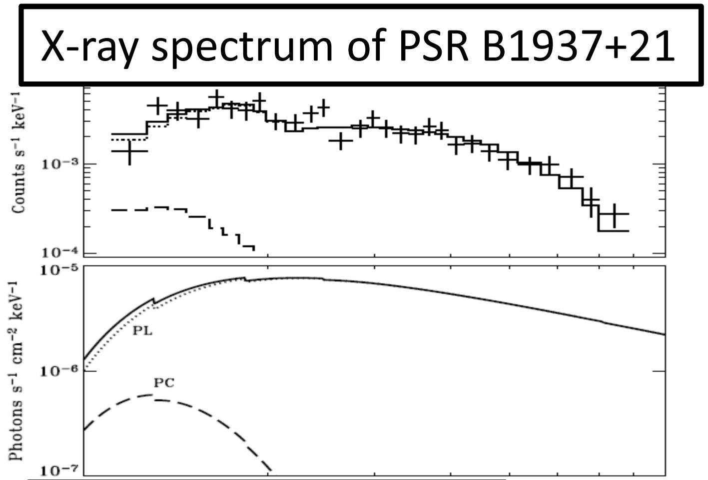

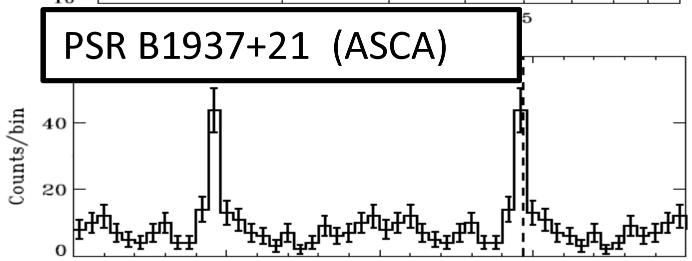

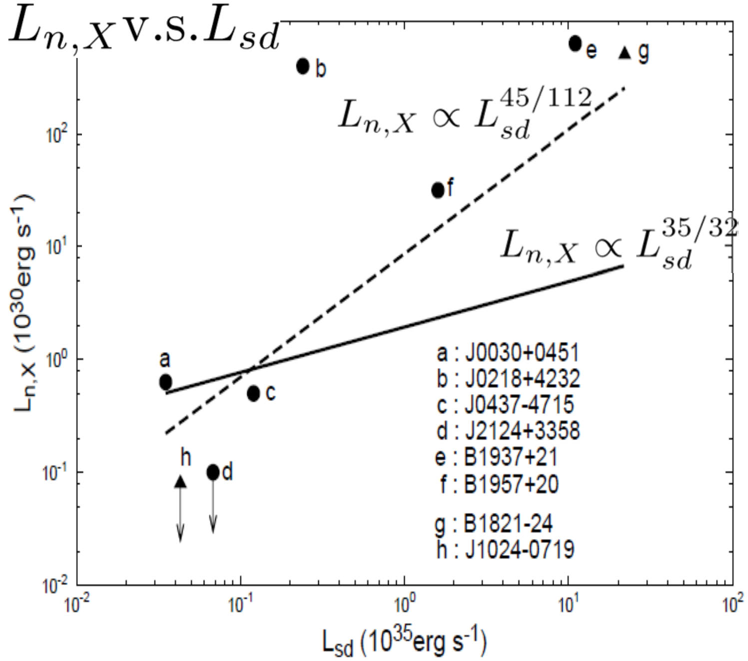

Non-thermal X-rays

- ❑ ～6 MSPs also exhibit pulsed non-thermal X-ray emissions (Zavlin ,2007, *AP&SS*).
- ❑ The synchrotron emissions from pairs created by photon-photon pair-creation process in the outer magnetosphere.
- Optical depth

$$\tau_{X\gamma} \sim \frac{L_r \bar{\sigma}_{X\gamma}}{4\pi R_{lc} c k T_r} \quad \sim 0.002(L_{sd}/10^{34} erg\ s^{-1})^{9/16}(B_d/10^8 G)^{-27/8}$$

L_r; luminosity of the polar cap thermal emission

$\sigma_{X\gamma}$; cross section

- Luminosity $L_{n,X} \sim \tau_{X\gamma} L_\gamma$

1, Photon-photon pair-creation controls the gap,

$$L_{n,X} \sim 5 \times 10^{29} (L_{sd}/10^{35} \mathrm{ergs}^{-1})^{45/112} (B_d/10^8 \mathrm{G})^{-11/56} \mathrm{erg\ s}^{-1}$$

2, Magnetic pair-creation controls the gap

$$L_{n,X} \sim 6 \times 10^{30} K^{15/4} (L_{sd}/10^{35} \mathrm{ergs}^{-1})^{35/32} (B_d/10^8 \mathrm{G})^{3/8} \mathrm{erg\ s}^{-1}$$

Future…

- *Fermi* second pulsar catalog includes 40 MPs, which provide more good statistic test for the theoretical models.
- More information of non-thermal X-ray data are required to discuss both X-ray/γ-ray emission simultaneously.
- Class II MSPs are Crab-like pulsars (?)

-radio and gamma-ray peaks are in phase.

3, High-energy emissions of binary MSPs

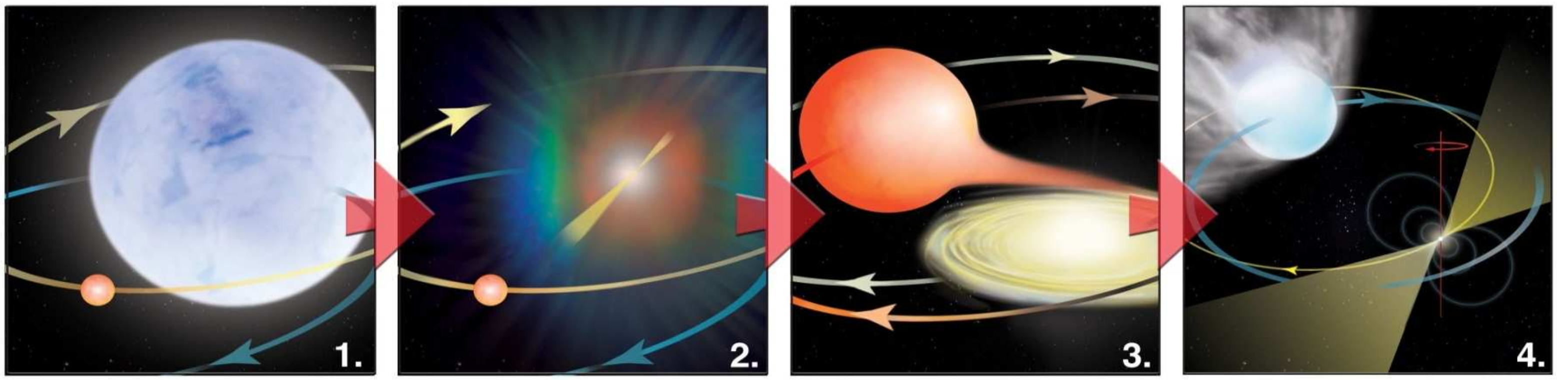

- ❑ Recycled scenario; MSPs are accreting spin-up pulsars by their low mass companions.
- ❑ Discovery of first accreting X-ray MSP (Wijnans & Van der Klis 1998, *Nature*)
- ❑ The new born radio MSP, FIRST J1023+0038; an example transiting from AXMPs to a rotation powered MSPs (Archibald et al. 2009, Sci).
- ❑ Discovery more black widow pulsars at Fermi un-ID sources (Roberts et al. 2011)
- ❑ The high-energy emissions associated with rotation powered activities of binary MSPs have been revealed.

AXMPs in quiescent state

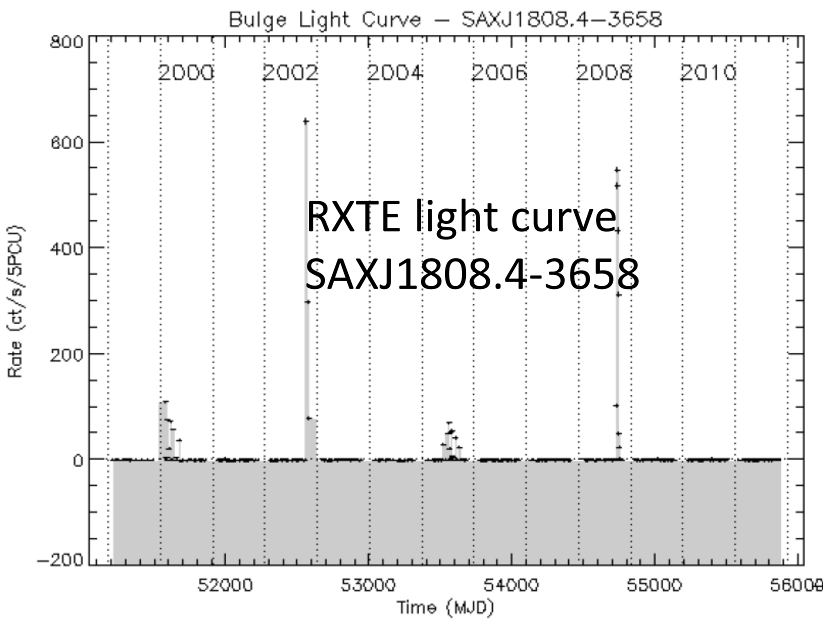

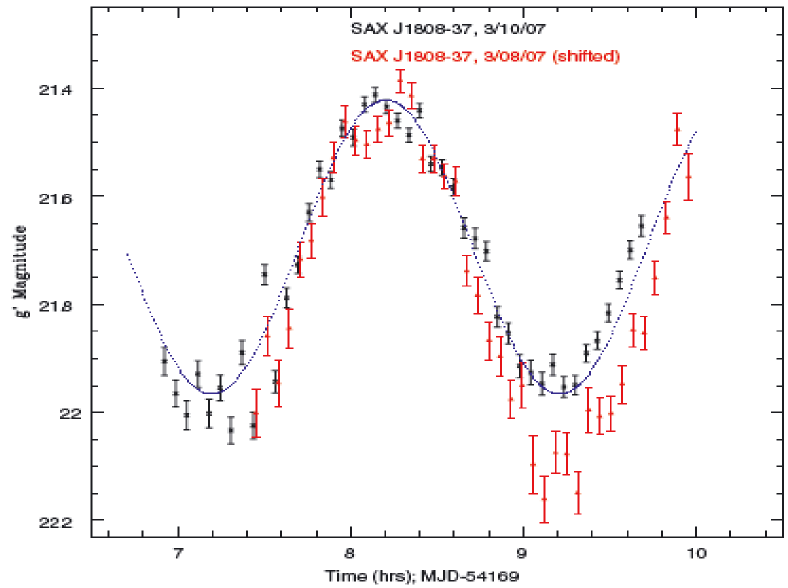

(SAX J1808-37 Deloye et al. 2008 *MNRAS*)

- ❑ The optical orbital modulations are found in quiescent state.

→ An incident luminosity of ~10^{34} erg/s; excluding the irradiation of the disk.

→ Irradiation of the pulsar wind (Burderi et al. 2003, *A&A*).

- ❑ Non-thermal X-ray emissions in quiescent sate (Heinke et al. 2009, *ApJ*) .
- ❑ The powered rotation activities are turned on in quiescent state.

New born MSP; J1023.4+0038

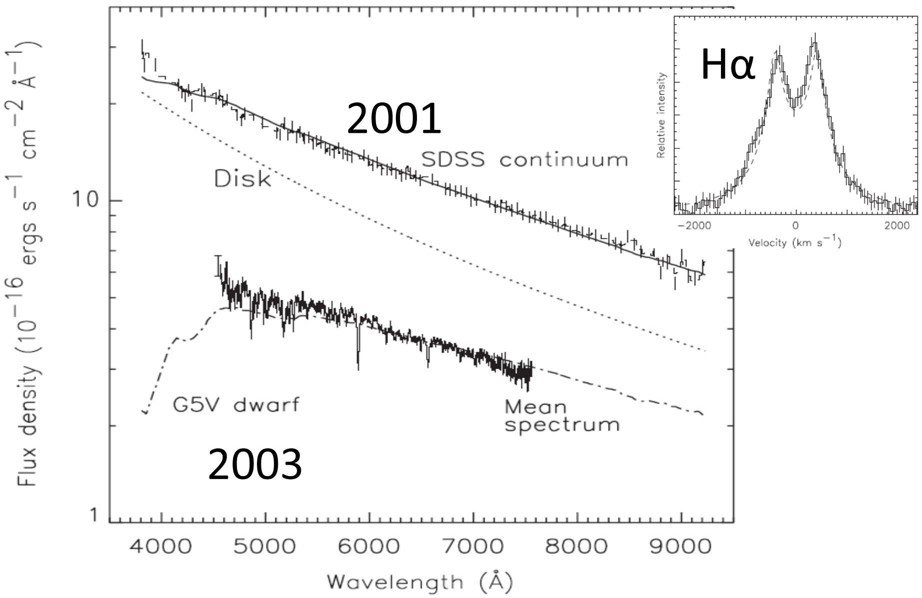

- Evidence (hydrogen and helium line emissions) of truncated accretion disk in 2001, and no pulsed radio emissions (Wang et al. 2009, *ApJ*)

- No evidence of disk in 2003 and pulsed radio emissions (Archibald et al. 2009 *Sci*).

- We detected non-thermal X-ray and gamma-ray emissions (2FGL J1023.6 + 0040; Tam et al. 2010, *ApJL*)

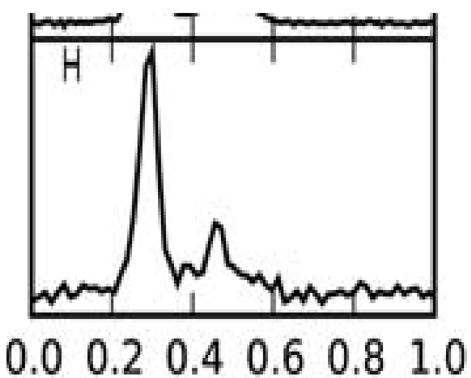

Radio pulse profile

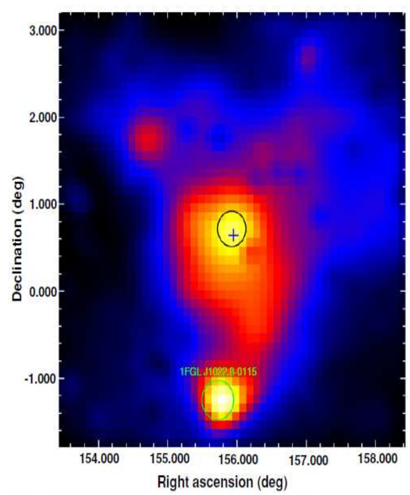

Test-Statistical map of 2FGL J1023

Model on J1023.4+0038 (Takata et al. 2010, *ApJL*)

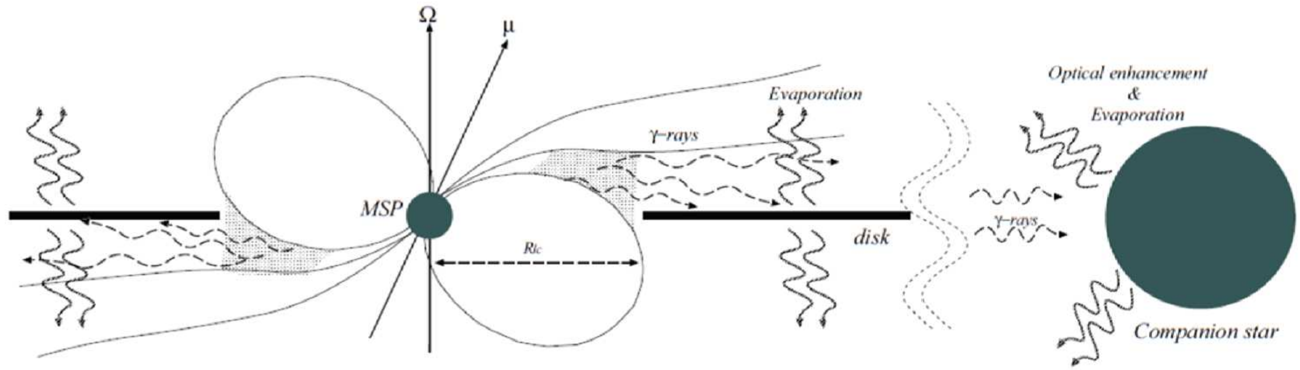

- ❑ J1023.4 +0038 is now in quiescent state.
- ❑ The rotation powered activities were already turned on in 2001.

- matter from the disk/companion absorb/scatter the pulsed radio emissions.

- ❑ Irradiation of γ-rays from the outer gap evaporated the disk.

-γ-rays are absorbed via the pair-creation process in Coulomb field

-The created pairs transfer their energy and momentum to the disk matter, and evaporate the disk .

$$\tau \sim 1 \left(\frac{\eta L_\gamma}{6 \cdot 10^{31}\ \mathrm{erg/s}}\right)^{-1} \left(\frac{r}{10^{10}\ \mathrm{cm}}\right)^{-1} \left(\frac{M_d}{10^{23}\ \mathrm{g}}\right) M_{1.4}\ \mathrm{yr},$$

Skin depth of low frequency EMW is too short compared with the disk thickness

Relativistic pulsar wind particles penetrate the disk.

- ❑ The rotation powered activities will be turned off after the system reenters the active state.

Black widow pulsars

-destroying the their companion

-link between binary MSPs and solitary MSPs.

- ❑ The first black widow pulsar PSR B1957+20 (Fruchter et al. 1988, *Nature*)

- Companion mass; ～0.025 solar mass.

- Radio eclipse with 10% orbital phase.

- Optical orbital modulation.

(T_{max}=8300K, T_{min}=2900K, Reynolds et al. 2007, *MNRAS*)

- ❑ The non-thermal X-ray emissions could be produced by the intra-binary shock (Arons & Tavani 1993, *ApJ*)

- ❑ Discovery of unresolved X-ray emissions (Stappers et al. 2003, *Sci*.)

- ❑ Pulsed X-ray and γ-ray emissions (Guillemot et al. ApJ, *2012*)

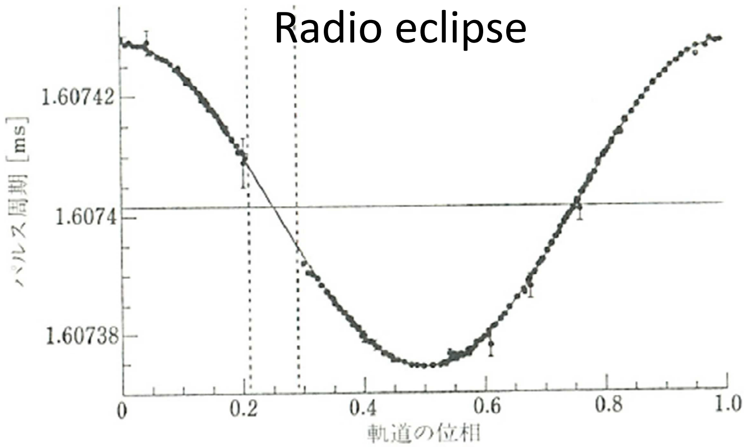

図 1 連星ミリ秒パルサー PSR 1957+20 のドップラー曲線 [A. S. Fruchter, D. R. Stinebring and J. H. Taylor: Nature 333 (1988) 237]

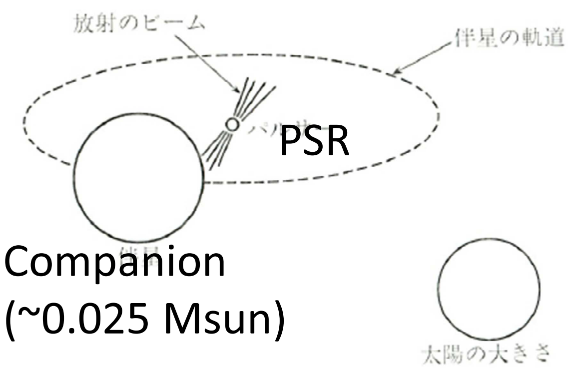

図 2 PSR 1957+20 を含む連星系の模式図

Credit by Shibazaki

New X-ray observation

(Huang et al. 2012, *submitted*)

Folded X-ray light curve (2 orbital cycle)

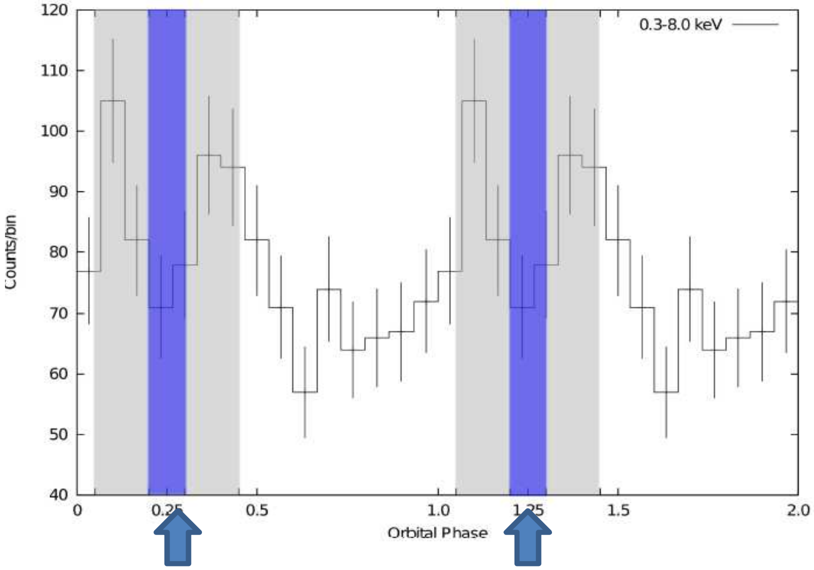

Inferior conjunction (Radio eclipse)

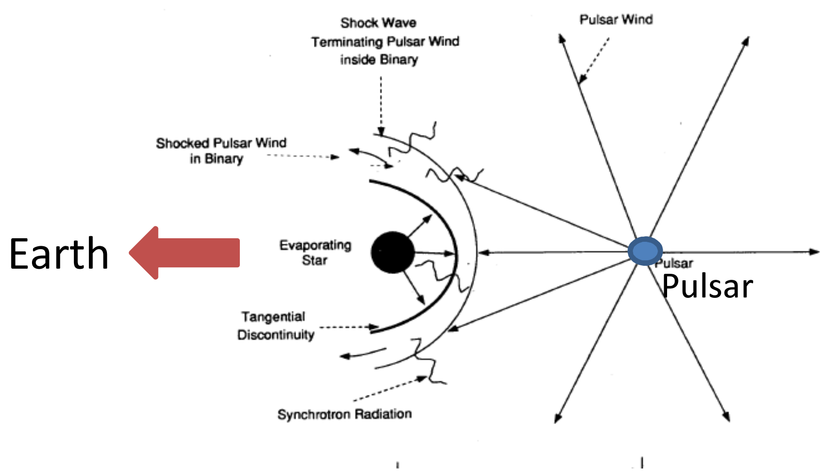

- ❑ 169ks Chandra observations
- ❑ Folded light curve at the orbital period (∼9.1 hrs =33ks) shows the orbital modulations.
- ❑ Emissions tend to increase around the inferior conjunction.
- ❑ Doppler boosting of the emissions from the post-shock flow with v∼ 0.2-0.3c.

Orbital phase dependent γ-ray spectrum

(Wu et al. 2012, *submitted*)

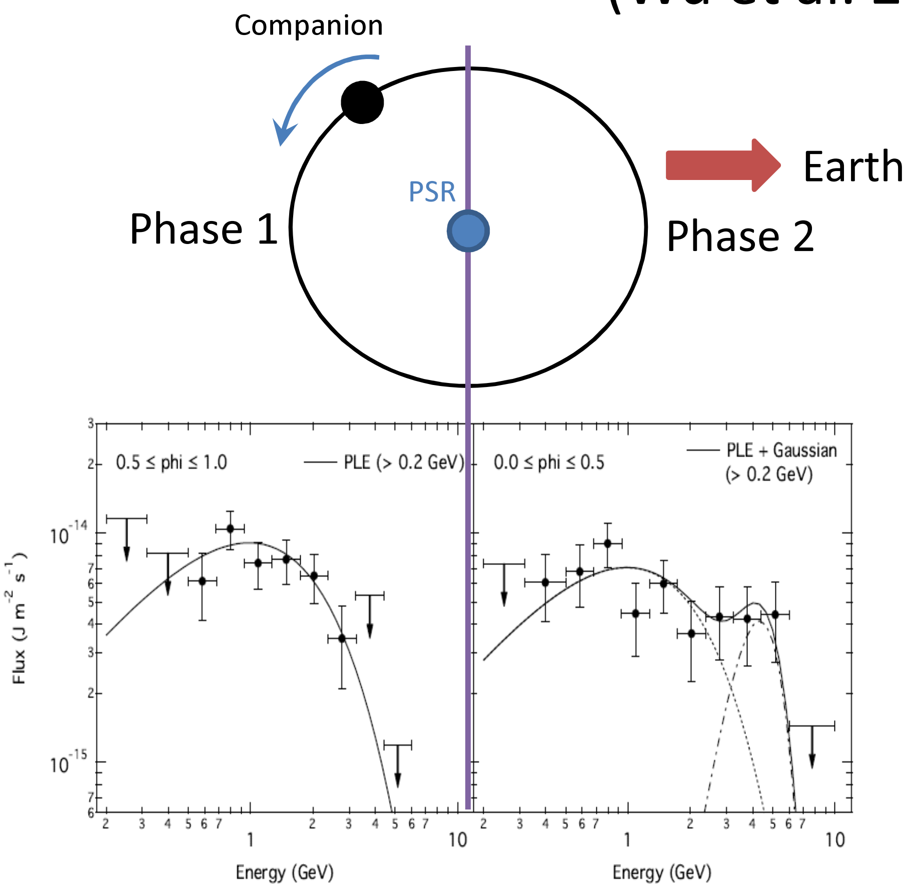

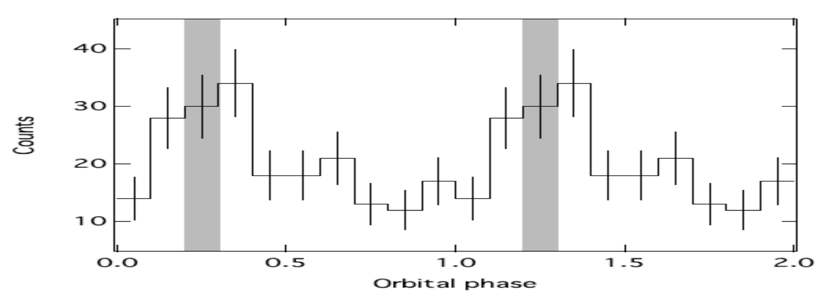

- ❑ 3yr *Fermi* data
- ❑ Divided the data into two parts

Phase1, half orbit centered at superior conjunction

Phase2, half orbit centered at inferior conjunction

- ❑ Spectrum

Phase 1; Typical pulsar spectrum

Phase 2; Additional component above 3GeV (～7σ)

- ❑ Evidence of the orbital modulation in folded light curve above 3~GeV.

Emissions from a cold relativistic pulsar wind?

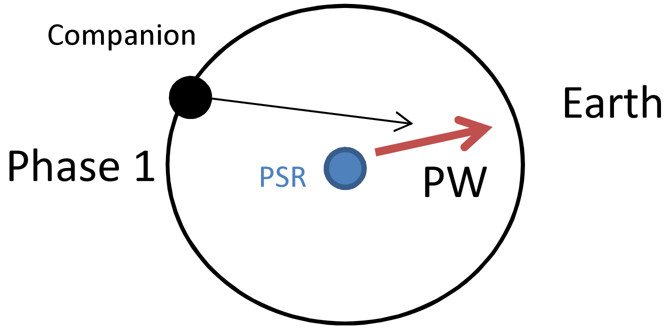

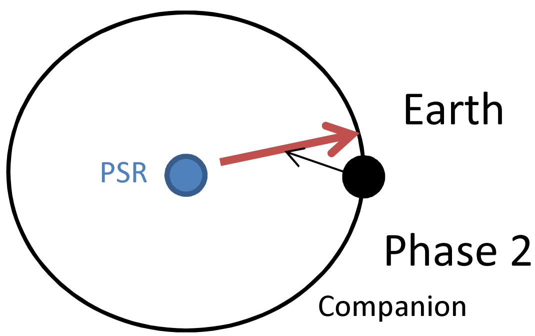

- It is unlikely the inverse-Compton process of the shocked wind;

$$F_\gamma/F_X >> U_p/U_B$$

- The IC process of a cold relativistic wind

- Emissivity is sensitive to the collision angle between the cold wind and soft photons
- Around superior conjunction (Phase 1); tail-on like collision and inefficient IC.
- Around inferior conjunction (Phase 2); head-on like collision and efficient IC.

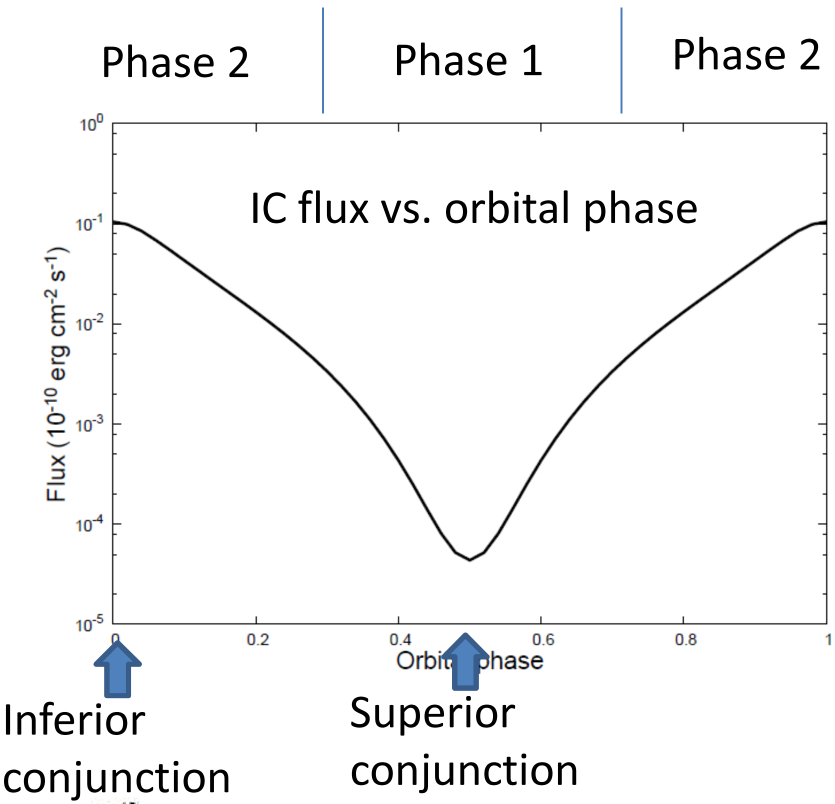

- ❑ Temperature of heated side of companion star, 8300K
- ❑ Assumption
- Pulsar wind carries the spin down power.
- Mono-energetic particle distribution, $\Gamma \sim 5 \times 10^4$

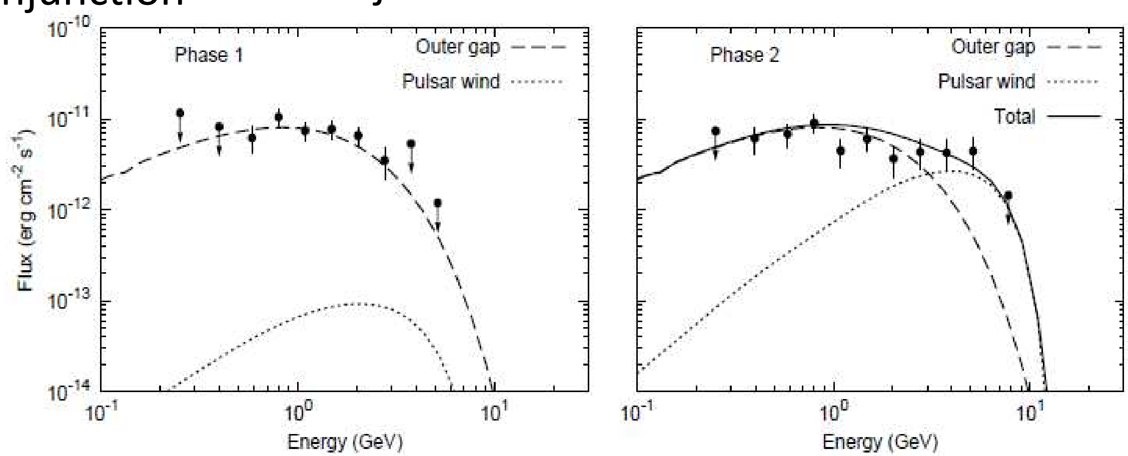

- ❑ PSR J2241-5236 is the anther candidate

Radio quiet MSPs?

- No radio-quiet MSPs have been found

- ~40 new radio MSPs at *Fermi* un ID sources

- Many radio quiet MSPs could contribute to *Fermi* un-ID sources (Takata et al. 2011, *MNRAS*).

- How can we identified radio-quiet MSPs at Fermi ID sources?

- observational challenging

-understanding the Galactic gamma-ray sources (TeV-cosmic ray source? Kisaka and Kawanaka , 2012, *MNRAS*)

Candidate

Source selection

- ❑ Bright Fermi un-ID source (>10^{-11} erg/cm 2 /s)
- ❑ No radio emissions are reported.
- ❑ High galactic latitude |b|>40 deg., which excludes the contribution of normal pulsars (Takata et al. 2011, *MNRAS*)
- ❑ Spectrum properties are similar with those of pulsars.

-steady and spectral cut-off at GeV.

γ-ray spectrum (1FGL J2339)

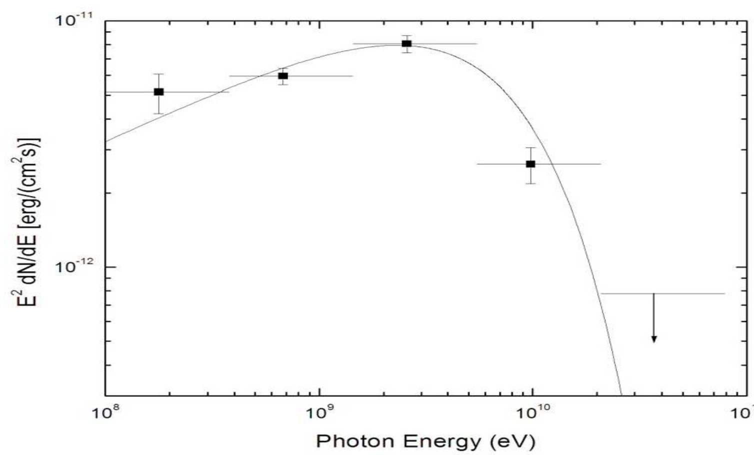

1FGL J2339.7-0531 (2FGL J2339.6-0532) is the best candidate for radio quiet MSP.

Multi-wavelength observations

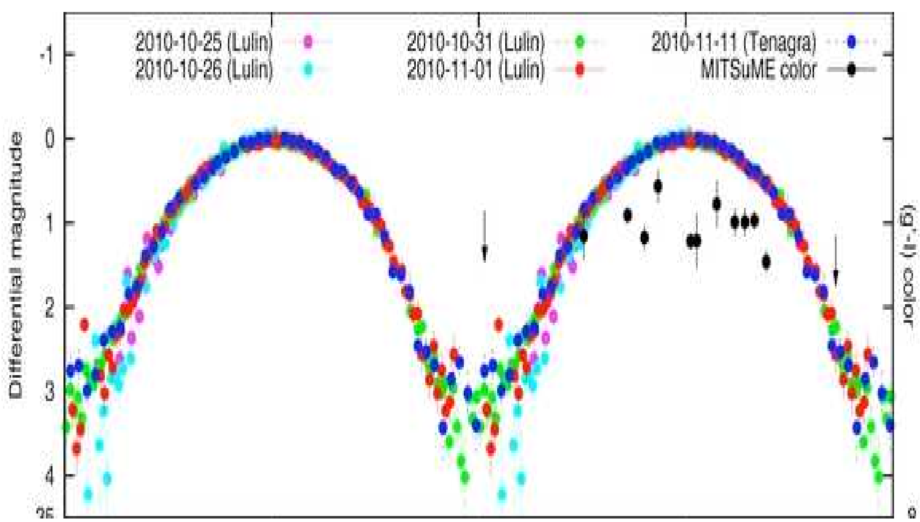

(Kong, et al. 2012, *ApJL)*

- Optical
  - -large variation (3-4 mag) with Pb～4.6hr
  - → binary system

parameter	fitted result
M_{CP}	0.059 M_{sun}
M_{CO}	1.4 M_{sun} ← fix
inclination	58 degree
Teff of CP	2100±50 K
log[Lx] (erg/s)	34
T_hotspot	6900K

(Yen, et al. 2012)

SUZAKU observations

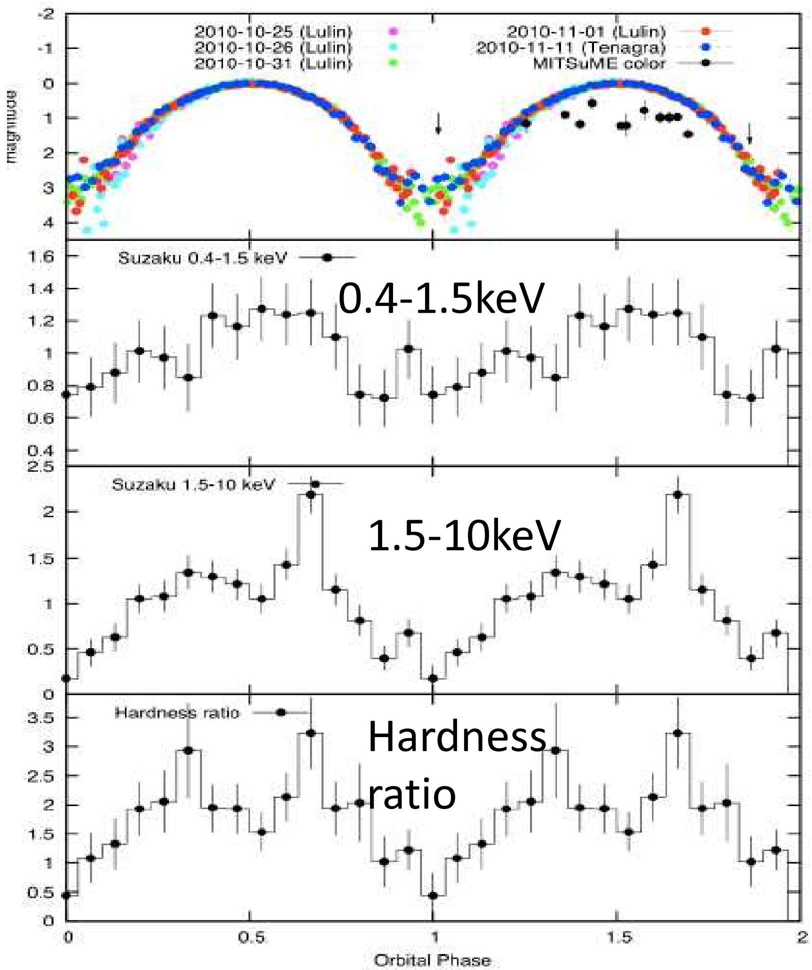

(Kong, et al. 2012)
(Takahasi et al. 2012)

- ❑ Hard X-rays; obvious modulation and non-thermal emissions
- → inter-binary shock

- ❑ Soft X-rays; stable and thermal component (kT～0.15keV and R ～1.6km)
- →heated polar cap of MSP

1FGL J2339.7-0531 is most likely radio-quiet black widow pulsar.

#2FGL J1311.7-3429 is the another source (Romani 2012, *ApJ*)

Radio quiet MSPs contribute to Fermi un-ID sources.

Future…

- ❑ Searching orbital modulating γ-ray emissions of binary MSPs

 - new born radio MSPs, radio-quiet MSP 1FGL J2339.7-0531 ….

 - study of emissions from cold pulsar wind

- ❑ Searching pulsed emissions from 1FGL J2339.7-0531 using X-ray data

- Searching pulsed emissions in LAT data is possible. But it is too difficult (Saz Parkinson 2012).

- ❑ More X-ray data

- Orbital phase-resolved spectra.

- Doppler boosting vs. physical eclipse ?

Conclusion 1

- The Fermi LAT has detected many MSPs (>40).

→testing on the emission models

- The outer gap controlled by the magnetic pair-creation process explains high-energy emissions from MSPs.

- Discoveries of high-energy emissions of new born radio MSP.

→ Indications of the rotation powered activities of AMXPs in quiescent state.

→ Irradiation of γ-ray can evaporate the disk.

Conclusion 2

- ❑ Discovery of the orbital phase dependent γ-ray spectra of original black widow pulsar PSR B1957+20.

→New window to study a cold pulsar wind.

- ❑ Multi-wavelength observations have revealed the radio-quiet black widow pulsars at the *Fermi* un-ID sources.

- ❑ More γ-ray emitting MSPs are waiting to be detected.

→Understanding actual distributions of γ-ray sources.

Before *Fermi*

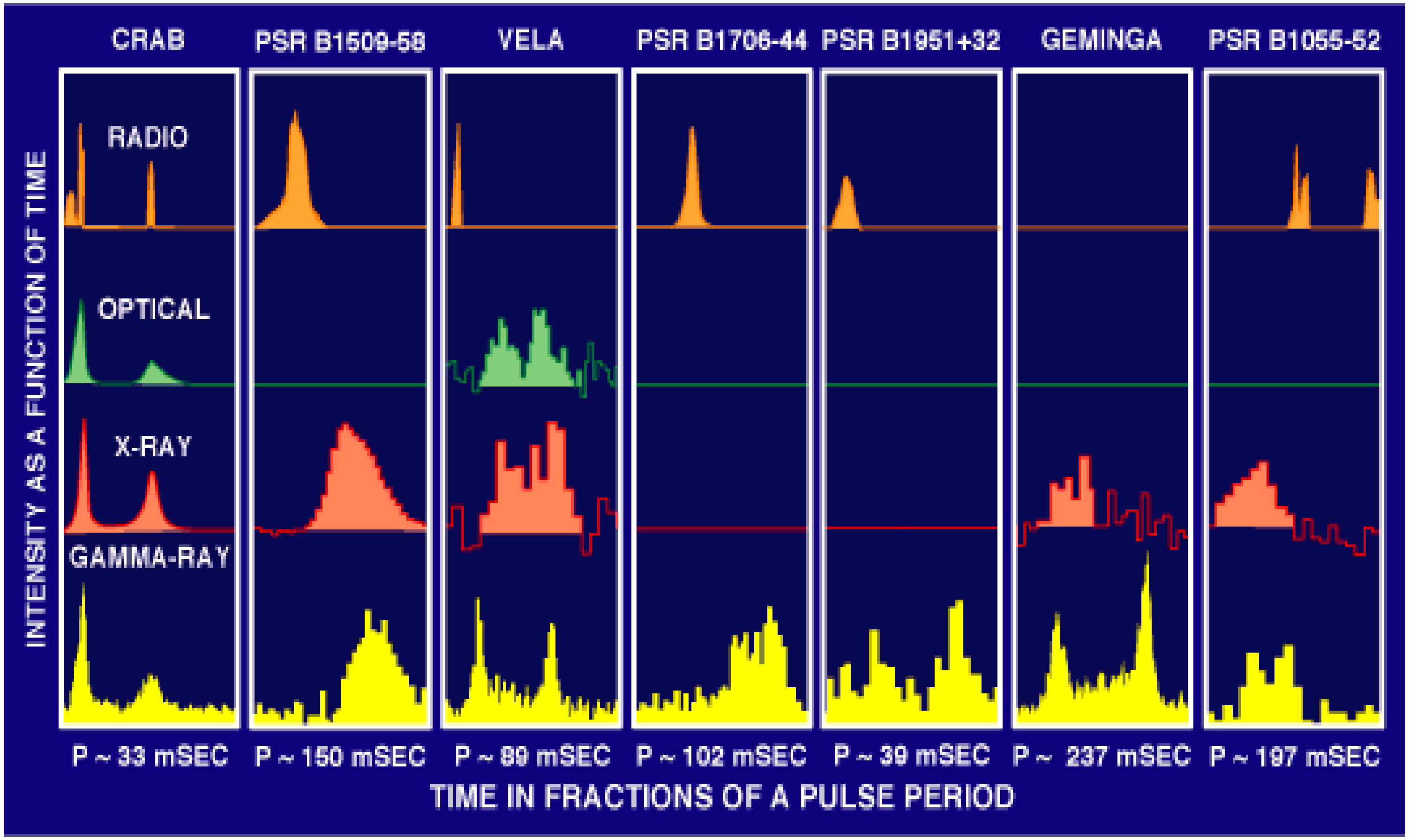

- Only 7 γ-ray pulsars were known in *EGRET* era
- Only 1 radio-quiet pulsar (GEMIGA) was known
- No γ-ray emitting MSPs was found.

Emissions from outer magnetosphere

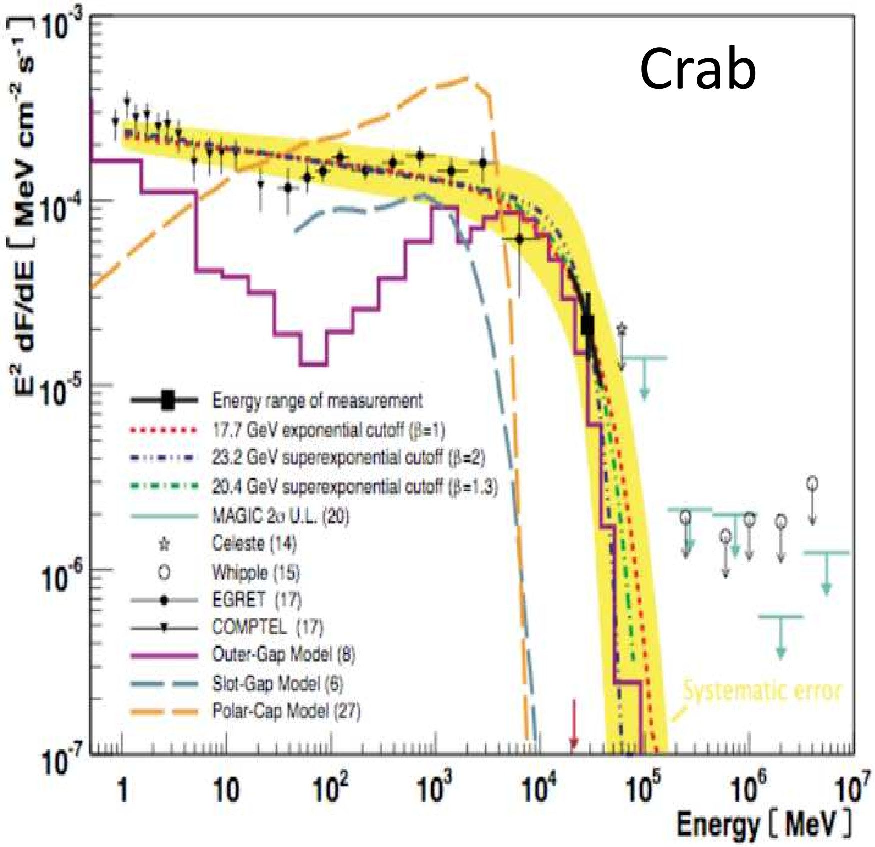

(Aliu et al. 2008, 2011 *Sci.*)

- ❑ Observed exponentially cut-off spectrum
- ❑ Polar cap
- Strong magnetic field produces super exponentially cut-off (Baring, 2004, *AdSPR*)
- ❑ Outer gap/slot gap
- Exponential cut-off
- ❑ Crab ~100GeV emissions are also favored by the magnetospheric emissions

X-ray tails

Chandra image

Hα image (green curves; X-ray contour)